Partial Proton Transfer in the Nitric Acid Trihydrate Complex

ARTICLE *in* THE JOURNAL OF PHYSICAL CHEMISTRY A · OCTOBER 2009

Impact Factor: 2.69 · DOI: 10.1021/jp9063033 · Source: PubMed

Partial Proton Transfer in the Nitric Acid Trihydrate Complex

Galen Sedo,[†] Jamie L. Doran, and Kenneth R. Leopold*

Department of Chemistry, University of Minnesota, 207 Pleasant Street SE, Minneapolis, Minnesota 55455

Received: July 3, 2009; Revised Manuscript Received: September 4, 2009

Four isotopologues of the gas-phase complex $HNO_3-(H_2O)_3$ have been observed by microwave spectroscopy in a supersonic jet. Rotational and nuclear electric quadrupole coupling constants have been obtained and the experimentally derived inertial defect has been used to infer a near-planar geometry for the complex. The data identify the observed species from among several structures predicted by theory, favoring a 10-membered ring geometry with the HNO_3 hydrogen-bonded to the first water, a series of water−water hydrogen bonds, and ring completion with the third water acting as a hydrogen-bond donor to an unprotonated HNO_3 oxygen. This structure corresponds to the lowest energy form predicted computationally in several prior studies as well as in this work using the MP2/6-311++G(2df,2pd) level/basis set. Although its observation does not rigorously establish its status as the lowest energy form, the concurrence between the predicted low-energy conformer and that observed in the ultracold supersonic jet strongly suggests that it is indeed the minimum-energy structure. The a-type spectra show evidence of internal dynamics, likely resulting from large amplitude motion of one or more of the water subunits. This complex represents the third step in the sequential hydration of HNO_3, and both the theoretical structure and experimental ^{14}N quadrupole coupling constants have been used to track the degree of ionization of the acid as function of hydration number. Based on ^{14}N quadrupole coupling constants, transfer of the HNO_3 proton to its nearest water molecule is about one-third complete in the trihydrate.

Introduction

An interesting fundamental question in chemistry concerns the role of solvent in stabilizing the ionized forms of simple protic acids. While many approaches to this problem can be envisioned, one involving the study of small gas phase clusters offers a simple and appealing point of view. The sequential addition of water molecules to an acid, for example, combined with a search for evidence of ionization within the resulting clusters, allows the dissociation to be studied as a solution is built up one molecule at a time. Information obtained regarding molecular and electronic structure offers a detailed view of the solvent−solute interactions that operate on a microscopic scale and, in doing so, provides an important part of the overall picture of solvation and ionization.

With this idea in mind, a variety of methods have been used to elucidate the relationship between proton transfer and solvation in small hydrated clusters. Infrared,[1−11] microwave,[12−23] NMR,[24,25] mass spectrometric,[26] and ultrafast[27,28] techniques, for example, have been employed, and numerous theoretical investigations have also been reported.[29−48] Perhaps most closely related to this work are microwave spectroscopic studies of gas phase complexes such as $HX-(H_2O)$ and $HX-(H_2O)_2$, (X = Cl[12,15] and Br[13,17]), HNO_3-H_2O,[14] $HNO_3-(H_2O)_2$,[18] $H_2SO_4-H_2O$,[19,20] $HCOOH-(H_2O)_n$ (n = 1−3),[21] CH_3COOH-H_2O,[22] and $CF_3COOH-(H_2O)_n$ (n = 1−3).[23] Overall, it now seems clear that for most simple acids, clustering with one or two waters is insufficient to promote ionization. Rather, at least three (and often more than three) water molecules are required before the potential energy surface develops a minimum corresponding to a hydrated ion pair. Even in preionized clusters, however, evidence of impending ionization can be discerned on the basis of structural and/or spectroscopic data.[14,18]

This work is concerned with the sequential hydration of nitric acid, whose ionization is represented by the well-known chemical reaction of eq 1.

$$HNO_3(l) + H_2O(l) \rightarrow NO_3^-(aq) + H_3O^+(aq) \qquad (1)$$

In the aqueous phase, comparison of the Raman intensities of alkali nitrates and aqueous HNO_3 solutions indicates significant variation in the percent ionization of the acid as a function of concentration and temperature. In a 1:3 mole ratio mixture of HNO_3 and H_2O at 298 K, for example, the percent dissociation is 51%, while in a 1:20 HNO_3/H_2O mixture at 278 K, 98% of the acid is dissociated.[49] In the solid state, on the other hand, crystallographic data indicate that the mono-, di-, and trihydrates are all fully ionic.[50−53] In contrast, what is not currently known is the number of water molecules needed to induce ionization in a small molecular cluster. Infrared studies suggest that the minimum number may be as low as three in amorphous thin films of HNO_3 and H_2O,[2] but for the gas phase complexes, more recent computational work indicates that four waters are needed before a solvated ion pair becomes even a local minimum on the potential energy surface.[1,41] In this case, however, the global energy minimum still corresponds to a hydrogen-bonded system, and further addition of water is needed in order to favor the formation of a microsolvated ion pair.[41]

Previous work in our laboratory has focused on microwave investigations of nitric acid mono- and dihydrates,[14,18] whose experimentally determined geometries are shown in Figure 1. Our studies of these systems concluded that, although signs of impending ionization are evident, both complexes are composed of hydrogen-bonded, neutral moieties, in good agreement with virtually all existing computational predictions. The present work

* To whom correspondence should be addressed. E-mail: kleopold@umn.edu.
[†] Present Address: Department of Chemistry, University of Manitoba, Winnipeg, Manitoba, Canada R3T 2N2.

10.1021/jp9063033 CCC: $40.75
Published on Web 09/29/2009

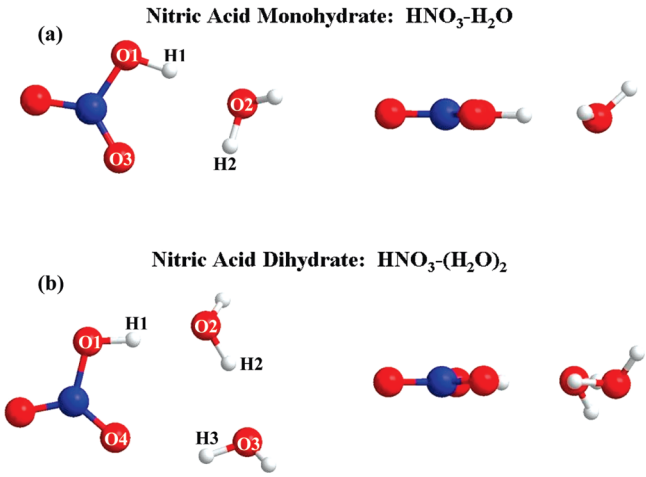

Figure 1. (a) The experimentally determined structure of HNO_3-H_2O from ref 14, top view (left), side view (right). (b) The experimentally determined structure of $HNO_3-(H_2O)_2$ from ref 18, top view (left), side view (right).

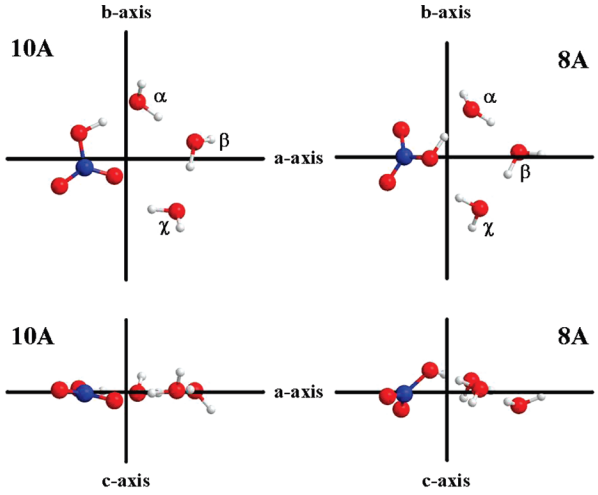

Figure 2. Theoretical structures for the lowest energy 10-member-ring (left) and 8-member-ring (right) nitric acid trihydrate conformers calculated in this work using the MP2/6-311++G(2df,2pd) level of theory and basis set. These structures are very similar to those previously reported in ref 1, 4, and 41. See text for discussion. The Greek letters α, β, and χ are used to label the water molecules.

endeavors, through a combination of experiment and theory, to further track the evolution of nitric acid ionization with cluster size via addition of a third water "solvent" molecule.

Several interesting features of the nitric acid−water system, and particularly the trihydrate, are worth noting. First, the structures shown in Figure 1 represent the only isomeric forms predicted by theory for the mono- and dihydrates. As cluster size increases, however, the possibility of isomerism arises, and for nitric acid−water complexes, the trihydrate is the smallest system for which more than one isomer has been predicted. In particular, for $HNO_3-(H_2O)_3$, two low-lying structures have been identified, and indeed there has been a bit of uncertainty as to which represents the lowest-energy form. The pertinent theoretical work on this system will be reviewed in a later section. However, at this point, we note that for both predicted isomers of the trihydrate, the cyclic motif persists but ring size differs. Figure 2 shows the basic geometries, in which different atoms of the HNO_3 participate in the hydrogen bonding, forming either a 10-membered ring with a near-planar array of heavy atoms and hydrogen bonds (2a), or a highly puckered 8-membered ring (2b). The microwave spectrum of the $HNO_3-(H_2O)_3$ reported in this work clearly establishes the observed species to be the 10-membered ring of Figure 2a.

Finally, there is considerable interest in nitric acid hydrates[54,55] and the phase behavior of HNO_3/H_2O mixtures[51,56−58] in the context of atmospheric chemistry. The formation of HNO_3 can create a temporary reservoir for atmospheric NO_x or conversely lead to its permanent removal through deposition in the troposphere[54] and denitrification in the stratosphere.[59,60] Moreover, uptake of atmospheric HNO_3 into sulfate aerosols, the formation of supercooled ternary solutions, and the crystallization of nitric acid trihydrate (NAT) are all central to current models of polar stratospheric cloud formation.[55] These clouds play a major role in the atmospheric chlorine cycle and, consequently, their formation directly impacts mechanisms for stratospheric ozone depletion. While the mechanism for the formation of solid nitric acid trihydrate in the atmosphere is still uncertain, there has been considerable discussion of the possibility that crystallization occurs at the gas−solution interface between air and aqueous droplets.[61−65] Moreover, the presence of stable molecular HNO_3 on the surface of binary (HNO_3-H_2O) and ternary ($HNO_3-H_2O-H_2SO_4$) solutions[66−69] has been established. Thus, a detailed description of the interactions between nitric acid and a limited number of water molecules may also play a role in understanding the formation of polar stratospheric clouds and hence in further elucidating mechanisms for the destruction of stratospheric ozone.

Experimental Methods and Results

Rotational spectra were recorded using a pulsed-nozzle Fourier transform microwave (FTMW) spectrometer[70] in which the free induction decay following coherent microwave excitation of molecules in a supersonic jet is recorded and Fourier transformed. Details of the apparatus have been provided elsewhere.[71] The nitric acid trihydrate complex was formed using an experimental setup similar to that employed in our investigations of both the mono- and dihydrates.[14,18] Argon carrier gas was passed through a sample of concentrated HNO_3 at room temperature and the resulting vapor was pulsed at a stagnation pressure of 2.5 atm through a 0.8 mm nozzle into the vacuum chamber. Although the local temperature in the expansion is difficult to measure by FTMW spectroscopy, rotational temperatures on the order of 2 K or less are typical.[70,72] To increase the amount of water present in the expansion, 10 standard cubic centimeters per minute (sccm) of argon were bubbled through a sample of liquid water and continuously introduced along the axis of the jet via a stainless steel needle (0.016 in. diameter). It has previously been noted that both nitric acid mono- and dihydrates can be observed without incorporating this secondary water source (i.e., using the water already present in the nitric acid solution).[18] However, for all spectra of the trihydrate observed in this work, use of the continuous flow source was necessary to obtain acceptable signal-to-noise ratios.

The transition intensities for the $HNO_3-(H_2O)_n$, $n = 0-3$, series were observed to decrease, on average, about 2 orders of magnitude with the addition of each water moiety. This drop, though significant, was not prohibitive for any of the four isotopic species reported in this work, given sufficient signal averaging. After locating the parent spectrum, both $H^{15}NO_3$ and DNO_3 were synthesized "in house" from the reaction between the appropriate isotopically substituted forms of $NaNO_3$ and H_2SO_4,[73] and the corresponding spectra of the complex were readily observed. For $HNO_3-(H_2{}^{18}O)_3$, a sample of 97% $H_2{}^{18}O$ was used in conjunction with the continuous flow needle and

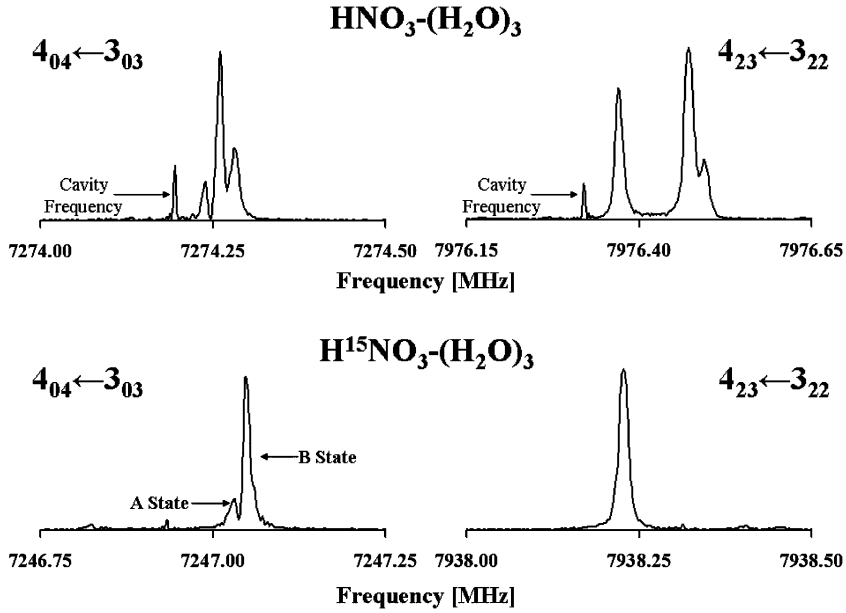

Figure 3. Sample spectra for the parent and ^{15}N isotopically substituted nitric acid trihydrate complex.

the spectra showed no significant decrease in intensity relative to those of the parent species. Attempts to observe the mixed $H_2{}^{16}O$ and $H_2{}^{18}O$ species using mixtures of $H_2{}^{16}O$ and $H_2{}^{18}O$ in the continuous flow source, however, were unsuccessful, likely a result of significant isotopic dilution from the eight possible $H_2{}^{16}O/H_2{}^{18}O$ forms of the complex. Similarly, the $HNO_3-(D_2O)_3$ species was not observed after switching the water source to 99.9% D_2O, in this case likely due to extensive hyperfine splitting of the six deuterium nuclei. No attempt was made to observe the mixed $H_2{}^{16}O/D_2{}^{16}O$ species given the possibility of 64 isotopologues, each with significant hyperfine structure. The frequencies employed in the final spectral analysis were collected using 1000−2000 gas pulses, with signals averaged over 6000−20000 free induction decays. Sample spectra for both the parent and the ^{15}N isotopically substituted complexes are shown in Figure 3.

The spectra in Figure 3 exhibit splittings analogous to those observed for both the mono- and dihydrated forms of nitric acid. For these systems, two types of spectral splitting were observed: (1) doubling arising from a pair of tunneling states associated with the internal motion of the water subgroups and (2) electric quadrupole hyperfine structure associated with the ^{14}N nuclear spin. The former is typical of water complexes of this type[14,15,17,18] and likely arises from interchange of equivalent water protons and/or wagging of the free water protons above and below the molecular plane. However, for reasons noted above, the deuterium substitutions necessary to more thoroughly characterize these motions were not carried out for the tridydrate.

For both the mono- and dihydrated complexes, spectra arising from each of the two tunneling states were analyzed separately, resulting in a fit of the lower frequency lines (arbitrarily labeled the "A State" fit) and a second fit of the higher frequency lines (arbitrarily labeled the "B State" fit). However, in the case of $HNO_3-(H_2O)_3$, low transition intensities in some cases caused the less intense components of the internal motion doublets to be unobservable. As a result, only a limited amount of data was collected for the A state, and only analysis of the more intense B state is presented in this paper. When both components of a doublet were observed, the less intense (A State) line was always located at a lower frequency than its B state partner. Note that the use of "A" in this context is intended to be analogous to the usage in our previous HNO_3-H_2O[14] and $HNO_3-(H_2O)_2$[18] work and should not be confused with the labeling of the structures "10A" and "8A" in Figure 2, where "A" is used to differentiate these structures from those discussed in a subsequent section.

For rotational transitions in which both the A and B states were observed, the size of the splitting was comparable to that arising from the ^{14}N electric quadrupole hyperfine structure (i.e., only on the order of a few hundred kilohertz). Thus, to avoid the possibility of initially assigning an A state line as one of the B state hyperfine components, assignments were first completed on the transitions where no A state was observed in the ^{15}N isotopic species (for which the hyperfine structure is absent). This procedure was used for both the parent and triple $H_2{}^{18}O$-substituted complexes. In the case of $DNO_3-(H_2O)_3$, congestion due to the deuterium electric quadrupole coupling made it necessary to fit the rotational transitions to their approximate line centers, with quoted uncertainties equal to the width of the transition at half its maximum intensity. In all cases, the rotational structure was analyzed using the semirigid rotor Hamiltonian, as it is expressed in eq 2,[74]

$$\mathbf{H} = \left[\frac{(B+C)}{2} - \Delta_J \mathbf{J}^2\right]\mathbf{J}^2 + \left[A - \frac{(B+C)}{2} - \Delta_{JK}\mathbf{J}^2 - \Delta_K \mathbf{J}_z^2\right]\mathbf{J}_z^2 + \left[\frac{(B-C)}{2} - 2\delta_J \mathbf{J}^2\right](\mathbf{J}_x^2 - \mathbf{J}_y^2) - \delta_K[\mathbf{J}_z^2(\mathbf{J}_x^2 - \mathbf{J}_y^2) + (\mathbf{J}_x^2 - \mathbf{J}_y^2)\mathbf{J}_z^2] \quad (2)$$

where A, B, and C are rotational constants, the $\mathbf{J}$s are angular momentum operators, and the upper- and lower-case deltas are centrifugal distortion constants. The ^{14}N nuclear quadrupole hyperfine structure of the parent and triply $H_2{}^{18}O$-substituted complexes were fit with the addition of an electric quadrupole coupling term containing the usual χ_{aa} and $(\chi_{bb} - \chi_{cc})$ coupling constants.[74] The nitrogen nuclear spin, $\mathbf{I}_N$, was coupled to the rotational angular momentum, $\mathbf{J}$, to produce the total angular momentum, $\mathbf{F} = \mathbf{I}_N + \mathbf{J}$, and only transitions in which $\Delta F = +1$ were observed. The splittings between these hyperfine components rapidly decrease with increasing J and inclusion

TABLE 1: Spectroscopic Constants of the Nitric Acid Trihydrate Complex[a]

	$HNO_3-(H_2O)_3$	$HNO_3-(H_2{}^{18}O)_3$	$H^{15}NO_3-(H_2O)_3$	$DNO_3-(H_2O)_3$
A	2269.2958(33)	2090.7418(26)	2268.3900(55)	2246.4960(66)
B	1215.91165(47)	1150.91574(43)	1209.02260(65)	1210.2466(12)
C	798.28664(29)	748.13110(26)	795.19691(39)	792.93040(44)
Δ_J	0.0010561(43)	0.0009517(52)	0.0010550(90)	0.0010900(93)
Δ_{JK}	−0.002266(25)	−0.001933(29)	−0.002340(76)	−0.002780(75)
δ_j	0.0004094(27)	0.0003776(40)	0.0004100(62)	0.0004260(58)
δ_k	0.000840(28)	0.000802(20)	0.000840(13)	0.000847(12)
χ_{aa}	−0.7993(67)	−0.7939(40)		
$\chi_{bb}-\chi_{cc}$	0.387(12)	0.4004(76)		
σ (rms)[b]	0.0048	0.0030	0.0021	0.0034
κ[c]	−0.4322	−0.4000	−0.4382	−0.4258

[a] All values, except for the asymmetry parameter, κ, are in MHz. Values in parentheses are one standard error in the least-squares fit. All symbols have their usual meanings. See ref 74. [b] Root mean squared residual in the least-squares fit. [c] κ is the asymmetry parameter, defined by $\kappa \equiv (2B - A - C)/(A - C)$.

of higher K_{-1} rotational transitions ($K_{-1} \leq 4$ and 3 for the parent and triple $H_2{}^{18}O$-substituted species, respectively), where the hyperfine splittings were more pronounced, was necessary for an accurate determination of both hyperfine constants. All spectra were fit using the SPFIT program of Pickett.[75] A complete list of the transition frequencies for each of the isotopic species studied is provided as Supporting Information. Also included are the residuals from the nonlinear least-squares fit, which generally fell within the estimated experimental uncertainties. The resulting spectroscopic constants are given in Table 1.

It may be seen from Table 1 that inclusion of transitions involving higher values of K_{-1} resulted in the need to incorporate four centrifugal distortion constants into the rotational Hamiltonian. The three parameters, Δ_J, Δ_{JK}, and δ_j, were necessary to achieve adequate residuals. However, similar results could be obtained using either Δ_K or δ_k as the fourth distortion constant. In the case of the $H^{15}NO_3$ and DNO_3 species (where only transitions with $K_{-1} \leq 2$ were included), Δ_K and δ_k could be omitted completely with no substantive changes in the other fitted constants, and only slight increases in the calculated residuals. To maintain consistency from one isotopologue to the next, the constants in Table 1 and the calculated frequencies provided in the Supporting Information are the result of fitting δ_k and omitting Δ_K, effectively setting the latter to zero in eq 2.

Seventy-four a-type transitions were included in the analysis of the parent $HNO_3-(H_2O)_3$ complex. A careful search for b-type rotational transitions was carried out, but none were observed. Given the low intensities of the observed a-type transitions and a predicted projection of the total dipole moment onto the b-inertial axis that is approximately one-fifth of its projection onto the *a*-axis, our inability to observe the b-type transitions was not unforeseen. No attempt was made to observe c-type transitions, and no transitions were observed that could be attributed to predicted spectra for 8A.

Note from Table 1 that despite the absence of observed b- and c-type rotational lines, the A rotational constants for the isotopic forms studied are well determined. This arises from the significant asymmetry of the complex: As seen in Table 1, the value of Ray's asymmetry parameter,[74] $\kappa \equiv (2B - A - C)/(A - C)$, is approximately −0.4. This is quite far from the limiting value of −1 for a prolate rotor, and thus the A constant can be determined with reasonable accuracy from the a-type spectra alone.

Theoretical Methods and Results

McCurdy et al.[1] were the first to report a cyclic structure for the gaseous $HNO_3-(H_2O)_3$ complex, similar to that labeled 10A in Figure 2. Their structure, calculated using second-order Møller−Plesset perturbation theory (MP2) and the aug-cc-pVDZ basis set, contains a series of hydrogen bonds resulting in a ring that incorporates 10 atoms, 6 covalent bonds, and 4 hydrogen bonds. Subsequent density functional theory calculations by Escribano et al.[4] found two low-energy structures using the Becke three-parameter hybrid functional with Lee, Yang, and Parr correlation (B3LYP) and the aug-cc-pVTZ basis set. The first is a nonplanar 10-member ring, similar to that of McCurdy et al., whereas the second contains the third water acting as a proton donor back to the hydroxyl oxygen of the nitric acid. This latter configuration results in a highly puckered ring comprising only eight atoms, four covalent bonds, and four hydrogen bonds (similar to 8A in Figure 2). The hydrogen bonds in this structure were described as "weaker and more twisted than in the favored configuration", and the calculations placed it about 0.8 kcal/mol higher in energy than the 10-membered ring. However, a later study by Scott and Wright[41] found that this energy ordering could be reversed depending on the theoretical method employed. In particular, B3LYP/6-311++G(2d,p) calculations showed qualitative agreement with those of Escribano et al., placing the 10-member ring conformer ∼0.1 kcal/mol lower in energy, but MP2 calculations with the same basis set resulted in an 8-member ring that was ∼0.4 kcal/mol lower in energy than the corresponding 10-member ring.

Given the very small energy differences and the agreement between the B3LYP calculations of Scott and Wright[41] and Escribano et al.,[4] we decided to take another look at the conformers 10A and 8A at the MP2 level of theory using the 6-311++G(2df,2pd) basis set. This choice was made in order to include both adequate polarizing functions needed to treat the strong primary hydrogen bond and diffuse functions necessary to model the weaker intermolecular interactions associated with the second and third water units. As a check, the structures of the mono- and dihydrates were also calculated. Table 2 compares the intermolecular bond lengths obtained for the HNO_3-H_2O and $HNO_3-(H_2O)_2$ with those determined experimentally and demonstrates that reasonable results may be expected from this level of theory and basis set. Full sets of Cartesian coordinates for the MP2/6-311++G(2df,2pd) calculations are included in the Supporting Information. Table 2 also lists the intermolecular bond distances corresponding to the MP2/aug-cc-pVDZ structures of McCurdy et al.[1] for comparison. All of the calculations were performed using the Gaussian '03 (G03) program package.[76]

The MP2/6-311++G(2df,2pd) calculations readily reproduced the basic geometries for the 10-member and 8-member rings, though the structure for 10A appears to be somewhat more

TABLE 2: Comparison of Calculated Intermolecular Distances for HNO_3-H_2O and $HNO_3-(H_2O)_2$ with Experimental Values[a]

	HNO_3-H_2O			$HNO_3-(H_2O)_2$		
	exptl[b]	MP2/6-311++G(2df,2pd)[c]	MP2/ aug-cc-pVDZ[d]	exptl[e]	MP2/6-311++G(2df,2pd)[c]	MP2/ aug-cc-pVDZ[f]
R(H1−O2)	1.779(33)	1.696	1.713	1.643(76)	1.609	1.629
R(H2−O3)	2.30	2.363	2.39	1.806(15)	1.767	1.781
R(H3−O4)				2.045(52)	2.031	2.048

[a] All distances are in Å. Atom numbering refers to Figure 1. [b] Reference 14. [c] This work. [d] Reference 1. [e] Reference 18. [f] Calculated from Cartesian coordinates of ref 1 as reported in ref .

TABLE 3: Calculated Bond Lengths of the 10-Member and 8-Member Ring Conformers of $HNO_3-(H_2O)_3$[a]

	10A			8A		
	O−H (ring)	O−H (unbound)	O···H	O−H (ring)	O−H (unbound)	O···H
HNO_3	1.015		1.561	1.021		1.543
α H_2O	0.984	0.959	1.713	0.983	0.960	1.727
β H_2O	0.976	0.959	1.793	0.975	0.959	1.800
χ H_2O	0.965	0.959	1.957	0.967	0.959	1.982
free HNO_3		0.970			0.970	
free H_2O		0.959			0.959	
free H_3O^+		0.977			0.977	

[a] Geometries calculated using MP2/6-311++G(2df,2pd) level of theory and basis set. Hydrogen bonds are listed according to proton donor. For example, the hydrogen bond between nitric acid and the α water is listed under nitric acid, the hydrogen bond between the α and β waters is listed under α water, etc.

planar than that of Escribano et al. This near-planar geometry is similar to that of the mono- and dihydrates and is the structure shown in Figure 2A. The calculated structure for 8A is shown in Figure 2b. Frequency calculations were performed for both 10A and 8A and verified both to be true minima on the potential energy surface. The global minimum structure is determined to be 10A, with 8A lying 0.372 kcal/mol higher in energy, in qualitative agreement with the previous B3LYP and MP2/aug-cc-pVDZ calculations. Zero-point-energy corrections do not alter this ordering, with the unscaled zero-point corrected energy of 8a lying 0.312 kcal/mol above that of 10A. The binding energy of 10A relative to the separated monomers is 31.1 kcal/mol (24.0 kcal/mol with unscaled zero-point corrections). Table 3 provides a comparison of the important inter- and intramolecular bond distances for the two structures. A complete listing of Cartesian coordinates for both isomers is provided as Supporting Information, and a detailed comparison of ring angles and dihedral angles for the two structures may be found elsewhere.[22]

The hydrogen bonds in Table 3 are listed according to the proton donor, that is, the primary hydrogen bond between the nitric acid and the first water is listed under nitric acid. The Greek letters (α, β, and χ) are used to differentiate between the individual water units, as indicated in Figure 2. It may be seen from the table that the covalent O−H bonds within the ring of each isomer are elongated from their corresponding values in the free monomers. This increase is most pronounced in the nitric acid OH bond, which is elongated by 0.045 Å in 10A, and is calculated to decrease steadily around the ring, with the OH bond of the third (χ) water remaining nearly unchanged from that of the free monomer for both species. Similarly, the H···O hydrogen bond lengths of the two structures increase steadily along the ring. The primary hydrogen bond between the nitric acid proton and the (α) water oxygen is approximately 1.55 Å in both isomers, a value which is ∼0.4 Å shorter than the weakest hydrogen bond involving the (χ) water as the proton donor.

For both 10A and 8A, all of the hydrogen bonds are calculated to be shorter than the corresponding hydrogen bonds in the smaller hydrates. For example, for the MP2/6-311++G(2df,2pd) calculations, the primary hydrogen bond of 10A (i.e., HNO_3 to the α water) is 0.135 Å shorter than that in the monohydrate and 0.048 Å shorter that in the dihydrate (see Table 2). Similarly, the fourth hydrogen bond with the (χ) water donating back to the nitric acid, is calculated to be 0.406 Å shorter in 10A than the analogous ring-closing hydrogen bond in the monohydrate, and 0.074 Å shorter than that in the dihydrate.

The free-proton orientations of both 10A and 8A involve an alternating up−down−up arrangement. To explore how changes in this light atom orientation affect the optimized geometry, the 10-member ring structure was reoptimized with a series of different light atom orientations. Allowing the three free protons to lie either above or below a heavy atom plane results in four unique sets of orientations: (α↑β↓χ↑), (α↓β↑χ↑), (α↑β↑χ↓), and (α↑β↑χ↑), where the Greek letters, once again, refer to the water moiety and the arrows refer to the free proton's position above or below the ring plane. These configurations correspond to the starting geometries for a series of calculations which yielded the optimized global minimum structure (10A) as well as three new local minimum-energy structures shown in Figure 4 (labeled 10B, 10C, and 10D). As for 10A and 8A, frequency calculations were performed for 10B-D and no imaginary frequencies were found, indicating that they represent true potential energy minima. Once having established the 10-membered ring to be the form of the complex observed (see below), no effort was made to explore analogous conformers of the 8-membered ring, though it is certainly possible that such structures correspond to additional local minima on the potential surface. For 10B−D, the energies relative to the global minimum (10A) are 0.288 kcal/mol (10B), 0.489 kcal/mol (10C), and 0.977 kcal/mol (10D). Although not indicated in Figure 4, the covalent and hydrogen bond distances in structures 10B−D are similar to those of 10A, despite the obvious increase out-of-plane bending. Complete sets of Cartesian coordinates for these higher energy forms are also provided as Supporting Information. Note that the existence of these minima does not necessarily guarantee the existence of distinct vibrationally averaged structures. In HNO_3-H_2O, for instance, the zero point energy for the free-proton wagging motion is nearly the same as the barrier at the planar configuration, leading to the conclusion that the complex is best regarded as quasi-planar.[14] However,

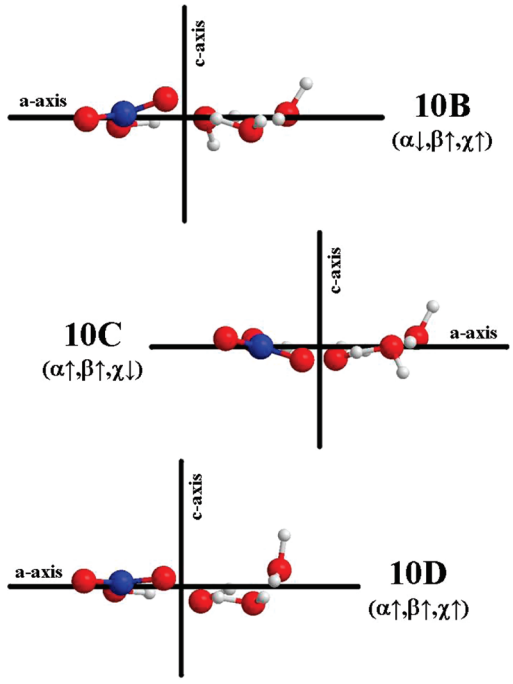

Figure 4. Local minimum structures for the 10-member ring nitric acid trihydrate conformer calculated using the MP2/6-311++G(2df,2pd) level/basis set.

since the barriers to interconversion between trihydrate structures were not computed, no statements can be made regarding the localization (or lack thereof) of the free protons in these minima.

Discussion

A. Identity of the Observed Conformer. The theoretical predictions of the previous section suggest that 10A is the lowest energy structure of $HNO_3-(H_2O)_3$, in agreement with the conclusions of most prior calculations. However, the computed energy differences between 10A and a variety of alternate structures are small. According to the results of this study, for example, 8A lies only 0.37 kcal/mol above the ground state, and thus the energy ordering determined by theory, while certainly suggestive, is not entirely unambiguous. Spectroscopic data, on the other hand, can be used to identify the structure observed experimentally, but it does not rigorously establish the ground state of the system. Fortunately, however, at the nominal 2K temperature of the supersonic jet, 0.37 kcal/mol is quite high in energy, corresponding to approximately 93 kT. Moreover, there is no a priori reason to expect that the low frequency vibrations capable of interconverting the various conformers and isomers would not efficiently cool. Thus, while neither theory nor experiment alone can unambiguously confirm that a given structure is the ground state of the system, any correspondence between the form observed in a cold supersonic jet and that with the lowest calculated energy provides strong evidence in favor of its identity as the true lowest-energy structure.

Although the four isotopologues studied in this work are not sufficient to determine a full experimental structure for the observed species, the data can be used to identify it from among the theoretical structures described above. Table 4 lists the observed minus calculated values of the rotational constants of the parent isotopologue, namely, A (obs − calcd), B (obs − calcd), and C (obs − calcd), for each of the theoretical structures considered. For the isotopically substituted species studied, the experimental *changes* in the rotational constants relative to the parent form (ΔA, ΔB, and ΔC) are compared with values calculated from the theoretical structures. The table further lists the calculated binding energies (relative to 10A), zero point corrected binding energies (relative to 10A), and the inertial defect, Δ_{ID}, defined by the first equality in eq 3.

$$\Delta_{ID} \equiv \frac{h}{8\pi^2}\left(\frac{1}{C} - \frac{1}{A} - \frac{1}{B}\right) = -2\sum_i m_i c_i^2 \qquad (3)$$

Here, A, B, and C are the system's rotational constants, h is Planck's constant, m_i are the atomic masses, and c_i is the c-coordinate of the ith atom in the inertial axis system of the complex, (a,b,c). The second equality in eq 3 follows from the definition of the rotational constants and holds in the absence of vibrations. For a planar molecule in which vibrational motion is negligible, the atoms always lie in the $a-b$ plane, and thus Δ_{ID} is zero. With increasing out-of-plane mass, however, Δ_{ID} becomes increasingly negative[74] and therefore serves as a measure of nonplanarity. Note that using the rotational constants of Table 1, the experimental inertial defect of the parent form of nitric acid trihydrate is determined to be −5.261 amu·Å^2. As a point of reference, comparable values for the mono-[14] and dihydrates[18] are −0.380 and −1.822 amu·Å^2, respectively. Thus, the magnitude of Δ_{ID} increases slightly from the mono- through the trihydrate, consistent with the addition of out-of-plane hydrogen atoms.

Examination of the computed inertial defects for the five theoretical structures of $HNO_3-(H_2O)_3$ reveals that 10A is a much better match to the experimental data than any of the others listed. The very large value of 8A reflects the extensive puckering of the ring (Figure 2) for that form, and the more modest values of 10B−D arise from a smaller, but still nonzero deformation of the ring from planarity (Figure 4). On the other hand, the small value for 10A arises largely from out-of-plane protons with small additional contributions from the heavy atoms. Large amplitude motion of the free water protons is expected to cause slight differences between the experimental inertial defect and the calculated equilibrium values and in this light, the agreement between the experimental and theoretical Δ_{ID} values of 10A is quite good. This further suggests that the experimental values of Δ_{ID} are not severely contaminated by vibrational motion.

It should be noted that direct comparison of the rotational constants and isotopic shifts is less informative. For example, while the calculated rotational constants for 10A are in reasonable agreement with the experimental values, the same is seen to be true for many (though perhaps not all) of the rotational constants calculated for 10B−D and 8A. Similarly, changes in rotational constants upon isotopic substitution for the ^{15}N, ^{18}O, and DNO_3 derivatives are in reasonable agreement with experiment for all the forms considered. This situation arises because the five theoretical structures are relatively similar to each other and thus A, B, and C, vary less among them than the expected accuracy of the calculations. Consequently, while the rotational constants and isotopic shifts confirm that the observed species is $HNO_3-(H_2O)_3$, they do not definitively link them to any of the calculated structures. The inertial defect, on the other hand, is able to assign the observed spectrum to that of 10A because it is a direct measure of out-of-plane mass and therefore highlights the structural feature for which the various calculated forms of the complex differ the most.

In summary, the calculated rotational constants as well as the predicted isotopic shifts are in good agreement with

TABLE 4: Comparison Between the Experimental Results and Theoretical[a] Predictions

	experimental	10A	10B	10C	10D	8A
ΔE [kcal/mol][b]		0	0.288	0.489	0.977	0.372
ΔE_{ZPC} [kcal/mol][b]		0	0.203	0.408	0.659	0.312
			$HNO_3-(H_2O)_3$			
A (obs − calcd) [MHz]		−33.004	−64.303	−27.195	−153.334	−219.160
B (obs − calcd) [MHz]		−39.410	−42.322	−35.927	19.868	−20.220
C (obs − calcd) [MHz]		−23.745	−40.643	−32.273	−36.230	−112.532
Δ_{ID} [amu·Å^2]	−5.261	−7.307	−15.815	−15.295	−25.555	−57.066
			$HNO_3-(H_2{}^{18}O)_3$			
ΔA [MHz]	−178.554	−181.743	−182.816	−179.172	−187.488	−183.659
ΔB [MHz]	−64.996	−67.408	−66.940	−67.534	−65.442	−65.828
ΔC [MHz]	−50.156	−52.122	−52.918	−52.472	−51.334	−57.179
Δ_{ID} [amu·Å^2]	−5.311	−7.345	−16.235	−15.906	−27.817	−59.080
			$H^{15}NO_3-(H_2O)_3$			
ΔA [MHz]	−0.906	−0.909	−0.649	−0.882	−0.924	−0.049
ΔB [MHz]	−6.889	−7.178	−7.276	−7.128	−6.846	−7.677
ΔC [MHz]	−3.090	−3.195	−3.305	−3.260	−3.425	−4.169
Δ_{ID} [amu·Å^2]	−5.259	−7.311	−15.828	−15.295	−25.572	−57.074
			$DNO_3-(H_2O)_3$			
ΔA [MHz]	−22.800	−21.657	−22.559	−21.499	−23.377	−13.388
ΔB [MHz]	−5.665	−2.032	−1.623	−1.986	−1.745	−1.508
ΔC [MHz]	−5.356	−3.637	−3.604	−3.700	−3.557	−0.984
Δ_{ID} [amu·Å^2]	−5.191	−7.311	−15.849	−15.295	−25.613	−58.064

[a] All calculations were performed using MP2/6-311++G(2df,2pd) level of theory and basis set, and the energies of the conformers are relative to that of 10A. For the parent form, A (obs − calcd), etc. are the differences between observed and calculated rotational constants. For the isotopically substituted forms, ΔA, ΔB, and ΔC are the change upon substitution relative to the parent species. [b] ΔE is the energy of the potential minimum relative to that for 10A. ΔE_{ZPC} is the unscaled zero-point corrected binding energy, also relative to 10A. The binding energy of 10A relative to separated monomers is 31.1 kcal/mol (24.0 kcal/mol with zero-point corrections).

experiment, establishing that the observed species is, indeed, $HNO_3-(H_2O)_3$. However, the rotational constants themselves do not clearly identify the conformer observed. The inertial defect, on the other hand, links the observed spectra to conformer 10A. According to the arguments given at the beginning of this section, therefore, it seems likely that the near-planar, 10-membered ring with an alternating up−down−up arrangement of the free water protons is the lowest energy form of the complex.

B. Degree of Proton Transfer. The literature contains a variety of methods for quantifying the degree of ionization in simple acid−base pairs.[77] In this section, we examine two methods that may be applied to the results of this work. The first is based on molecular structure and is similar to that we have employed previously[18] for HNO_3-H_2O and $HNO_3-(H_2O)_2$. The second takes advantage of the near-planarity of the $HNO_3-(H_2O)_n$ ($n = 1-3$) complexes and employs ^{14}N nuclear quadrupole coupling constants to assess the degree of ionization.

Structural Signature of Proton Transfer. As noted above, the primary hydrogen bond distance in $HNO_3-(H_2O)_n$ decreases with increasing hydration number. Although such a trend is suggestive of incipient proton transfer, a decrease in hydrogen bond length, alone, does not necessarily signify a concomitant release of the proton from the acid. Indeed, proton transfer across an O1−H···O2 hydrogen bond is accompanied by both a decrease in the intermolecular H···O2 distance *and* an increase in the covalent O1−H bond length. Thus, it is reasonable to define[78] a "proton transfer parameter", ρ, that incorporates both distances to assess the degree of proton exchange, namely,

$$\rho = (r_{OH}^{complex} - r_{OH}^{free}) - (r_{H\cdots O}^{complex} - r_{H\cdots O}^{free}) \qquad (7)$$

Here, $r_{OH}^{complex}$ and r_{OH}^{free} are the O1−H bond lengths of the proton donor in the complex and the free acid, respectively (e.g., the OH bond length of complexed and free HNO_3, respectively). $r_{H\cdots O}^{complex}$ is the hydrogen bond length in the complex (H···O2) and $r_{H\cdots O}^{free}$ is the H−O2 distance in the covalent species that would be formed in the event of complete proton transfer (e.g., the OH bond length in H_3O^+ for the complexes considered here). When proton transfer is minimal, the first term is small, giving a negative value of ρ, while a large degree of proton transfer renders the second term small and gives rise to a positive value of ρ. Equal proton sharing between the acid and the base corresponds to a value of $\rho = 0$.

TABLE 5: Proton Transfer Parameters and Quadrupole Coupling Constants for HNO_3 Hydrates and Related Species

	ρ (Å)	χ_{cc} (MHz)
HNO_3		−0.0773(51)[a]
HNO_3-H_2O	−0.78[b]	0.0749(45)[b]
$HNO_3-(H_2O)_2$	−0.64[c]	0.1489(45)[c]
$HNO_3-(H_2O)_3$	−0.54[d]	0.206(7)[d]
NO_3^-(aq)		0.656[e]

[a] Calculated from χ_{aa} and ($\chi_{bb} - \chi_{cc}$) of ref 82. [b] Data of ref 14. [c] Reference 18. [d] This work (theoretical value). [e] Reference 83.

Using the theoretical bond lengths in Table 3, the value of ρ for the interaction between the nitric acid and the (α) water in the 10A conformer of $HNO_3-(H_2O)_3$ is found to be −0.54 Å. The analogous values for $HNO_3-(H_2O)_2$ and HNO_3-H_2O are −0.64 and −0.78 Å, respectively.[14,18,79] Values for all three complexes are listed in Table 5. The negative signs indicate that these systems are best described as hydrogen-bonded, in agreement with all previous computations. The steady increase from the monohydrate to the trihydrate, however, provides a measure of the degree of incipient ionization with increasing cluster size. The variation of ρ with hydration number is illustrated graphically in Figure 5a.[80]

Proton Transfer from Nuclear Quadrupole Coupling. An alternate (and entirely experimental) measure of proton transfer

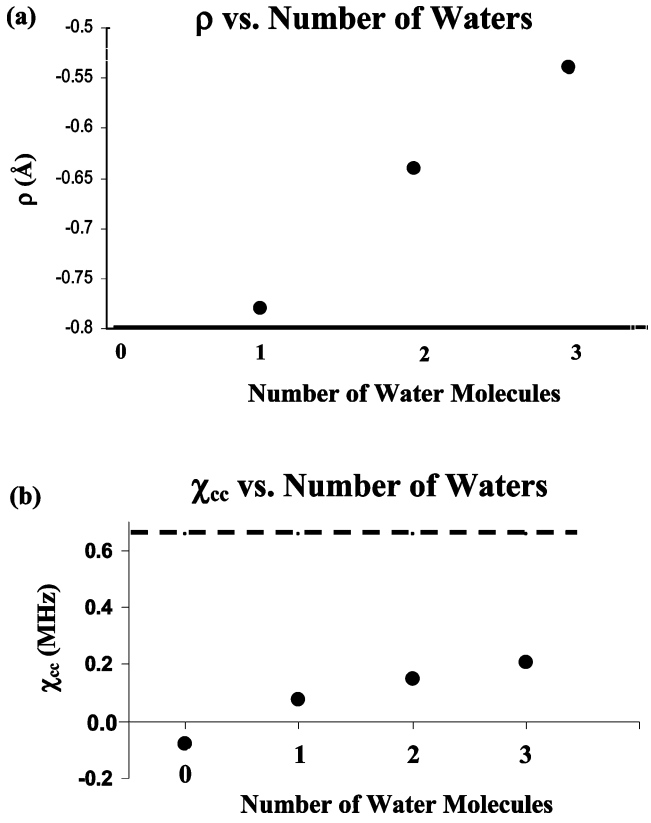

Figure 5. (a) ρ (in Å) vs the number of water molecules in $HNO_3-(H_2O)_n$ clusters. (b) χ_{cc} (in MHz) for the ^{14}N nucleus vs the number of water molecules in $HNO_3-(H_2O)_n$ clusters, HNO_3, and NO_3^-(aq). The dashed line represents the limiting value for NO_3^-(aq).

is available from ^{14}N nuclear quadrupole coupling constants. Since the components of the quadrupole coupling tensor for free nitric acid depend on the electric field gradient at the ^{14}N nucleus, χ_{aa}, χ_{bb}, and χ_{cc} intrinsically depend on the electronic structure of the HNO_3 itself. However, the coupling constants of the hydrates differ from those of free nitric acid because they are referred to the inertial axis systems of the complexes. As shown below, it is possible to analyze these constants in a way that separates the orientation dependence from the influence of electronic structure and thus provides information about the transition from hydrated HNO_3 to "solvated" NO_3^-.

In free nitric acid, the quadrupole coupling tensor has eigenvalues χ_{XX}, χ_{YY}, and χ_{ZZ}, and its principal axis system is designated (X,Y,Z), where Z lies perpendicular to the molecular plane. The orientation of the X and Y axes, as well as values of χ_{XX}, χ_{YY}, and χ_{ZZ} have been determined.[81,82] Moreover, since the mono-, di-, and trihydrates are very nearly planar, their c-inertial axes are essentially parallel to Z, that is, perpendicular to the HNO_3 or $HNO_3-(H_2O)_n$ plane, as shown in Figure 6. Thus the quadrupole coupling constants of the complex, χ_{aa}, χ_{bb}, and χ_{cc} are related to χ_{XX}, χ_{YY}, and χ_{ZZ} by a second rank tensor transformation corresponding to rotation about the Z axis, namely,

$$\chi_{aa} = \chi_{XX}\cos^2\theta + \chi_{YY}\sin^2\theta \tag{8}$$

$$(\chi_{bb} - \chi_{cc}) = \chi_{XX}(1 + \sin^2\theta) + \chi_{YY}(1 + \cos^2\theta) \tag{9}$$

$$\chi_{cc} = \chi_{ZZ} \tag{10}$$

where θ is the angle formed between the X-axis of free nitric acid and the a-inertial axis of the complex. The observed values of χ_{aa} and $(\chi_{bb} - \chi_{cc})$ are seen to depend on both the electronic structure of the HNO_3 (through their dependence on χ_{XX} and χ_{YY}) and the orientation of the HNO_3 within the complex (through their dependence on θ). χ_{cc}, on the other hand, depends on the electronic structure, but is independent of orientation.

Prior work has established that the X axis of the HNO_3 quadrupole coupling tensor lies in the HNO_3 plane, 1.88° off of the $N-O^H$ bond, rotated away from the hydrogen.[82] The eigenvalues $\chi_{XX} = 1.1468(34)$ MHz and $\chi_{YY} = -1.0675(34)$ MHz have also been determined.[82] Thus, to the extent that the HNO_3 remains electronically unaltered upon complexation, eqs 8 and 9 can be used to obtain values of $\theta = 110.4°$ and $\theta = 128.0°$ from the measured χ_{aa} and $(\chi_{bb} - \chi_{cc})$, respectively. These are in fair, though not excellent, agreement with the 100.2° value obtained from the theoretical structure for 10A. More importantly, however, the disparity between them suggests the quadrupole coupling constants of the complex are not purely projective and thus that small but significant changes in the HNO_3 have taken place upon complexation.

A simple measure of the changes in electronic structure of the HNO_3 can be developed using χ_{cc}. Exploiting the traceless character of the quadrupole coupling tensor,[74] values of χ_{cc} are readily obtained from the measured coupling constants given in Table 1, namely,

$$\chi_{cc} = -\frac{1}{2}[\chi_{aa} + (\chi_{bb} - \chi_{cc})] \tag{11}$$

According to eq 10 and the preceding arguments, if the HNO_3 remains unperturbed upon complexation, χ_{cc} should be independent of hydration number, as long as the complexes remain planar. Conversely, any observed change in χ_{cc} upon complex-

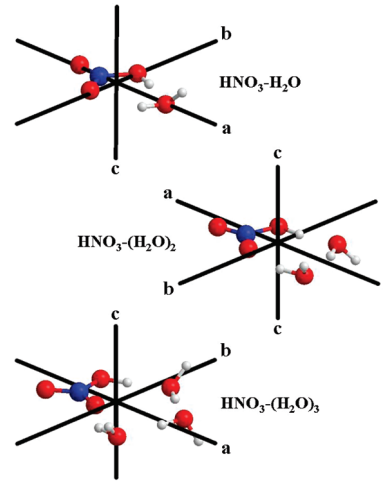

Figure 6. Orientation of the inertial axis systems for HNO_3-H_2O, $HNO_3-(H_2O)_2$, and $HNO_3-(H_2O)_3$. The Z axis of the HNO_3 quadrupole coupling tensor is perpendicular to the HNO_3 plane. The c axes for the complexes are parallel to Z and are clearly visible as the axis of rotation for the transformation between the (X,Y,Z) and (a,b,c) coordinate systems, where (a,b,c) is the inertial axis system of the complex.

ation reflects changes in the electronic structure as HNO_3 undergoes a transition to the NO_3^- anion. Values of χ_{cc} for $HNO_3-(H_2O)_n$ ($n = 0-3$) are listed in the second column of Table 5. Also given is a value for NO_3^-(aq) at infinite dilution at 25 °C determined by Adachi et al. using NMR relaxation times.[83,84] Because of the D_{3h} symmetry of the nitrate ion, this value also corresponds to an axis perpendicular to the NO_3^- plane and thus provides a limiting value for the case of complete ionization. A plot of χ_{cc} versus the number of water molecules is shown in Figure 5b, and a horizontal line is included in the figure to indicate the limiting value for NO_3^-. This method of using nuclear quadrupole coupling constants to asses proton transfer is similar to that employed by Legon and co-workers[85] for the C_{3v} symmetric amine hydrogen halides, but adapted here to account for the asymmetric nature of the nitric acid hydrates.

The measures of ionization provided by ρ and by χ_{cc} are strikingly similar. The latter has the advantage that limiting values for both HNO_3 and NO_3^- are well-defined, whereas limiting values of ρ for $NO_3^-H_3O^+$ and a hypothetical HNO_3-H_2O complex without proton transfer are not well determined. It is seen that for nitric acid complexed with three water molecules, χ_{cc} is about a third of the way between that of free HNO_3 and NO_3^-(aq), suggesting that the proton transfer might be described as "about a third complete". Further accuracy is probably not warranted, as there is no rigorous way to draw a boundary between proton donor and proton acceptor, and thus the "degree of proton transfer" is in some sense only defined by the method used to measure it. In this light, the similarity between ρ and χ_{cc} is all the more striking. Note, that although the dependence of χ_{cc} appears almost linear between zero and three waters, there is no reason to expect a linear dependence over the entire range between HNO_3(g) and NO_3^-(aq). Indeed, abrupt changes in the degree of ionization with hydration number are possible and thus no attempt to determine the minimum number of water molecules needed for ionization should be made by extrapolation of Figure 5.

Conclusions

The gas-phase complex $HNO_3-(H_2O)_3$ has been observed by Fourier transform microwave spectroscopy in a supersonic jet. Rotational and centrifugal distortion constants of four isotopic species have been determined, along with the ^{14}N quadrupole coupling constants for the parent and triply $H_2{}^{18}O$ substituted complexes. Analysis of the rotational constants identifies the observed conformer as that predicted to be the lowest energy form in several prior reports, as well as by MP2/6-311++G(2df,2pd) calculations in this work. This structure involves a nearly planar, 10-membered ring with the HNO_3 proton hydrogen-bonded to the first water, a series of water−water hydrogen bonds, and ring completion with the third water donating a hydrogen bond to an unprotonated HNO_3 oxygen. The observation of this form does not rigorously prove its identity as that with the lowest energy, but the low (~2 K) temperature of the supersonic jet, together with the absence of any additional spectra identifiable as those of other conformers or isomers, suggests that it is, indeed, the lowest energy structure. Spectral doubling is observed for some transitions and, by analogy with HNO_3-H_2O and $HNO_3-(H_2O)_2$, likely arises from internal motion involving one or more of the water units. The degree of proton transfer has been assessed using two methods, one based on molecular structure and a second which analyzes the electronic redistribution around the ^{14}N nuclei as revealed by nuclear quadrupole coupling constants. Both methods indicate that although the proton transfer is more advanced than in HNO_3-H_2O and $HNO_3-(H_2O)_2$, three water molecules are insufficient to fully ionize the acid. The nuclear quadrupole coupling data suggest that in the trihydrate, ionization of the HNO_3 moiety is about one-third complete.

Acknowledgment. This work was supported by the National Science Foundation (Grant No. CHE 0514256), the donors of the Petroleum Research Fund, administered by the American Chemical Society, and the Minnesota Supercomputer Institute.

Supporting Information Available: Tables of transition frequencies, assignments, and residuals for four isotopologues of $HNO_3-(H_2O)_3$ and Cartesian coordinates for computed structures. This material is available free of charge via the Internet at http://pubs.acs.org.

References and Notes

(1) McCurdy, P. R.; Hess, W. P.; Xantheas, S. S. *J. Phys. Chem. A* **2002**, *106*, 7628.
(2) Ritzhaupt, G.; Devlin, J. P. *J. Phys. Chem.* **1977**, *81*, 521.
(3) Huneycutt, A. J.; Stickland, R. J.; Helberg, F.; Saykally, R. J. *J. Chem. Phys.* **2003**, *118*, 1221.
(4) Escribano, R.; Couceiro, M.; Gómez, P. C.; Carrasco, E.; Moreno, M. A.; Herrero, V. J. *J. Phys. Chem. A* **203**, *107*, 651.
(5) Given, A.; Larsen, L. A.; Loewenschuss, A.; Nielsen, C. J. *J. Chem. Soc., Faraday Trans.* **1998**, *94*, 827.
(6) Couling, S. B.; Sully, K. J.; Horn, A. B. *J. Am. Chem. Soc.* **2003**, *125*, 1994.
(7) Couling, S. B.; Fletcher, J; Horn, A. B.; Newnham, D. A.; McPheat, R. A.; Williams, R. G. *Phys. Chem. Chem. Phys.* **2003**, *5*, 4108.
(8) Fárnik, M.; Weimann, M.; Suhm, M. A. *J. Chem. Phys.* **2003**, *118*, 10120.
(9) Ault, B. S.; Pimentel, G. C. *J. Phys. Chem.* **1973**, *77*, 57.
(10) Ritzhaupt, G.; Devlin, J. P. *J. Phys. Chem.* **1977**, *81*, 521.
(11) Barnes, A. J.; Lasson, E.; Nielsen, C. J. *J. Mol. Struct.* **1994**, *322*, 165.
(12) Kisiel, Z.; Pietrewicz, B. A.; Fowler, P. W.; Legon, A. C.; Steiner, E. *J. Phys. Chem. A* **2000**, *104*, 6970.
(13) Legon, A. C.; Suckley, A. P. *Chem. Phys. Lett.* **1988**, *150*, 153.
(14) Canagaratna, M.; Phillips, J. A.; Ott, M. E.; Leopold, K. R. *J. Phys. Chem. A* **1998**, *102*, 1489.
(15) Kisiel, Z.; Białkowska-Jaworska, E.; Pszczółokwski, L.; Milet, A; Struniewicz, C.; Moszynski, R.; Sadlej, J. *J. Chem. Phys.* **2000**, *112*, 5767.
(16) Kisiel, Z.; Kosarzewski, J.; Pietrewicz, B. A.; Pszczółkowski, L. *Chem. Phys. Lett.* **2000**, *325*, 523.
(17) Kisiel, Z.; Pietrewicz, B. A.; Desyatnyk, O.; Pszczółkowski, L.; Struniewicz, I; Sadlej, J. *J. Chem. Phys.* **2003**, *119*, 5907.
(18) Craddock, M. B.; Brauer, C. S.; Leopold, K. R. *J. Phys. Chem. A* **2008**, *112*, 488.
(19) Fiacco, D. L.; Hunt, S. W.; Leopold, K. R. *J. Am. Chem. Soc.* **2002**, *124*, 4504.
(20) Brauer, C. S.; Sedo, G.; Leopold, K. R. *Geophys. Res. Lett.* **2006**, *33*, L23805.
(21) Priem, D.; Ha, T.-K.; Bauder, A. *J. Chem. Phys.* **2000**, *113*, 169.
(22) Sedo, G. Ph.D. Thesis. University of Minnesota, Minnesota, 2008.
(23) Ouyang, B.; Starkey, T. G.; Howard, B. J. *J. Phys. Chem. A* **2007**, *111*, 6165.
(24) Limbach, H.-H. *Magn. Reson. Chem.* **2001**, *39*, (NMR Spectroscopy of Hydrogen-Bonded Systems; special issue, and references therein).
(25) Bango, A.; Scorrano, G. *Acc. Chem. Res.* **2000**, *33*, 609.
(26) Kay, B. D.; Hermann, V.; Castleman, A. W., Jr. *Chem. Phys. Lett.* **1981**, *80*, 469.
(27) Hurley, S. M.; Dermota, T. E.; Hydutsky, D. P.; Castleman, A. W, Jr. *J. Chem. Phys.* **2003**, *118*, 9272.
(28) Hurley, S. M.; Dermota, T. E.; Hydutsky, D. P.; Castleman, A. W., Jr. *Science* **2002**, *298*, 202.
(29) Thompson, W. H.; Hynes, J. T. *J. Phys. Chem. A* **2001**, *105*, 2582.
(30) Packer, M. J.; Clary, D. C. *J. Phys. Chem.* **1995**, *99*, 14323.
(31) Cabaleiro-Lago, E. M.; Hermida-Ramón, J. M.; Rodríguez-Otero, J. *J. Chem. Phys.* **2002**, *117*, 3160.
(32) Tao, F.-M.; Higgins, K.; Klemperer, W.; Nelson, D. D. *Geophys. Res. Lett.* **1996**, *23*, 1797.
(33) Al Natsheh, A. A.; Nadykto, A. B.; Mikkelsen, K. V.; Yu, F.; Ruuskanen, J. *J. Phys. Chem. A* **2004**, *108*, 8914.
(34) Re, S.; Osamura, Y.; Morokuma, K. *J. Phys. Chem. A* **1999**, *103*, 3535.
(35) Arstila, H.; Laasonen, K.; Laaksonen, A. *J. Chem. Phys.* **1998**, *108*, 1031.

(36) Bandy, A. R.; Ianni, J. C. *J. Phys. Chem. A* **1998**, *102*, 6533.
(37) (a) Weber, K. H.; Tao, F.-M. *J. Phys. Chem. A* **2001**, *105*, 1208. (b) Li, S.; Tao, F.-M.; Gu, R. *Chem. Phys. Lett.* **2006**, *426*, 1.
(38) Chaban, G. M.; Gerber, R. B.; Janda, K. C. *J. Phys. Chem. A* **2001**, *105*, 8323.
(39) Wei, D.; Truchon, J.-F.; Sirois, S.; Salahub, D. *J. Chem. Phys.* **2002**, *116*, 6028.
(40) Kuo, J.-L.; Klein, M. L. *J. Chem. Phys.* **2004**, *120*, 4690.
(41) Scott, J. R.; Wright, J. B. *J. Phys. Chem. A* **2004**, *108*, 10578.
(42) Salvador, P.; Szcześniak, M. *J. Chem. Phys.* **2003**, *118*, 537.
(43) Aloisio, S.; Hintze, P. E.; Vaida, V. *J. Phys. Chem. A* **2002**, *106*, 363.
(44) Mó, O.; Yáñez, M.; González, L.; Elguero, J. *Chem. Phys. Chem.* **2001**, *7*, 465.
(45) Wormer, P. E. S.; Groenenboom, G. C.; van der Avoird, A. *J. Chem. Phys.* **2001**, *115*, 3604.
(46) Milet, A.; Struniewicz, C.; Moszynski, R.; Sadlej, J.; Kisiel, Z.; Białkowska-Jaworska, E.; Pszczółkowski, L. *Chem. Phys.* **2001**, *271*, 267.
(47) Re, S. *J. Phys. Chem. A* **2001**, *105*, 9725.
(48) Chipot, C.; Gorb, L. G.; Rivail, J.-L. *J. Phys. Chem.* **1994**, *98*, 1601.
(49) See, for example:(a) Harned, H. S.; Owen, B. B. *The Physical Chemistry of Electrolytic Solutions*, 3rd ed.; Reinhold: New York, 1958. (b) Minogue, N.; Riordan, E.; Sodeau, J. R. *J. Phys. Chem. A* **2003**, *107*, 4436, and references therein.
(50) Delaplane, R. G.; Taesler, I.; Olovsson, I. *Acta Crystallogr.* **1975**, *B31*, 1486.
(51) Lebrun, N.; Mahe, F.; Lamiot, J.; Foulon, M.; Petit, J. C.; Prevost, D. *Acta Crystallogr. B* **2001**, *57*, 27.
(52) Lebrun, N.; Mahe, F.; Lamiot, J.; Foulon, M.; Petit, J. C. *Acta Crystallogr. C* **2001**, *57*, 1129.
(53) Taesler, I.; Delaplane, R. G.; Olovsson, I. *Acta Crystallogr.* **1975**, *B31*, 1489.
(54) Finlayson-Pitts, B. J.; Pitts, J. N., Jr., *Chemistry of the Upper and Lower Atmosphere*; Academic Press: San Diego, CA, 2000.
(55) Lowe, D.; MacKenzie, A. R. *J. Atmos. Solar-Terrestrial Phys.* **2008**, *70*, 13, and references therein.
(56) Beyer, K. D.; Hansen, A. R. *J. Phys. Chem. A* **2002**, *106*, 10275.
(57) Worsnop, D. R.; Fox, L. E.; Zahniser, M. S.; Wofsy, S. C. *Science* **1993**, *259*, 71.
(58) Tizek, H.; Knözinger, E.; Grothe, H. *Phys. Chem. Chem. Phys.* **2004**, *6*, 972.
(59) Tabazadeh, A.; Jensen, E. J.; Toon, O. B.; Drdla, K.; Schoeberl, M. R. *Science* **2001**, *291*, 2591.
(60) Waibel, A. E.; Peter, Th.; Carslaw, K. S.; Oelhaf, H.; Wetzel, G.; Crutzen, P. J.; Pöschl, U.; Tsias, A.; Reimer, E.; Fischer, H. *Science* **1999**, *283*, 2064.
(61) Knopf, D. A.; Koop, T.; Luo, B. P.; Weers, U. G.; Peter, T. *Atmos. Chem. Phys.* **2002**, *2*, 207.
(62) Tabazadeh, A.; Djikaev, Y. S.; Hamill, P.; Reiss, H. *J. Phys. Chem. A* **2002**, *106*, 10238.
(63) Djikaev, Y. S.; Tabazadeh, A. *J. Phys. Chem. A* **2004**, *108*, 6513.
(64) Knopf, D. A. *J. Phys. Chem. A* **2006**, *110*, 5745.
(65) (a) Tabazadeh, A. *J. Phys. Chem. A* **2007**, *111*, 1374. (b) Knopf, D. A. *J. Phys. Chem. A* **2007**, *111*, 1376.
(66) Yang, H.; Finlayson-Pitts, B. J. *J. Phys. Chem. A* **2001**, *105*, 1890.
(67) Kido Soule, M. C.; Blower, P. G.; Richmond, G. L. *J. Phys. Chem. A* **2007**, *111*, 3349.
(68) Shamay, E. S.; Buch, V.; Parrinello, M.; Richmond, G. L. *J. Am. Chem. Soc.* **2007**, *129*, 12910.
(69) Bianco, R.; Wang, S.; Hynes, J. T. *J. Phys. Chem. A* **2007**, *111*, 11033.
(70) Balle, T. J.; Flygare, W. H. *Rev. Sci. Instrum.* **1981**, *52*, 33.
(71) (a) Phillips, J. A.; Canagaratna, M.; Goodfriend, H.; Grushow, A.; Almlöf, J.; Leopold, K. R. *J. Am. Chem. Soc.* **1995**, *117*, 12549. (b) Phillips, J. A. Ph.D. Thesis. University of Minnesota, Minneapolis, MN, 1996.
(72) See, for example:(a) Arnó, J.; Bevan, J. W. In *Jet Spectroscopy and Molecular Dynamics*, Hollas, J. M., Phillips, D., Eds.; Blackie Academic & Professional: London, 1995. (b) Smalley, R. E.; Wharton, L.; Levy, D. H. *Acc. Chem. Res.* **1977**, *10*, 139.
(73) Chilton, T. H. *Strong Water Nitric Acid: Sources, Methods of Manufacture, and Uses*; MIT Press: Cambridge, MA, 1968; p 166.
(74) Gordy, W.; Cook, R. L. *Microwave Molecular Spectra*, 3rd ed.; John Wiley & Sons: New York, NY, 1984.
(75) Pickett, H. M. *J. Mol. Spectrosc.* **1991**, *148*, 371.
(76) , Frisch, M. J. Trucks, G. W. Schlegel, H. B. Scuseria, G. E. Robb, M. A. Cheeseman, J. R. Montgomery, J. A., Jr., Vreven, T. Kudin, K. N. Burant, J. C. Millam, J. M. Iyengar, S. S. Tomasi, J. Barone, V. Mennucci, B. Cossi, M. Scalmani, G. Rega, N. Petersson, G. A. Nakatsuji, H. Hada, M. Ehara, M. Toyota, K. Fukuda, R. Hasegawa, J. Ishida, M. Nakajima, T. Honda, Y. Kitao, O. Nakai, H. Klene, M. Li, X. Knox, J. E. Hratchian, H. P. Cross, J. B. Bakken, V. Adamo, C. Jaramillo, J. Gomperts, R. Stratmann, R. E. Yazyev, O. Austin, A. J. Cammi, R. Pomelli, C. Ochterski, J. W. Ayala, P. Y. Morokuma, K. Voth, G. A. Salvador, P. Dannenberg, J. J. Zakrzewski, V. G. Dapprich, S. Daniels, A. D. Strain, M. C. Farkas, O. Malick, D. K. Rabuck, A. D. Raghavachari, K. Foresman, J. B. Ortiz, J. V. Cui, Q. Baboul, A. G. Clifford, S. Cioslowski, J. Stefanov, B. B. Liu, G. Liashenko, A. Piskorz, P. Komaromi, I. Martin, R. L. Fox, D. J. Keith, T. Al-Laham, M. A. Peng, C. Y. Nanayakkara, A. Challacombe, M. Gill, P. M. W. Johnson, B. Chen, W. Wong, M. W. Gonzalez, C. Pople, J. A. *Gaussian 03,* revision C.02; Gaussian, Inc.: Wallingford, CT, 2004.
(77) See, for example:(a) Scheiner, S. *Hydrogen Bonding. A Theoretical Perspective*; Oxford Press: New York, 1997. (b) Jeffrey, G. A. *An Introduction to Hydrogen Bonding*; Oxford Press: New York, 1997.
(78) Kurnig, I, J.; Scheiner, S. *Int. J. Quantum Chem. Quantum Biol. Symp.* **1987**, *14*, 47 This definition was originally applied to amine−hydrogen halide complexes but is readily generalized for nearly linear hydrogen bonds, as in eq 7.
(79) The MP2/6-311++G(2df,2pd) values are−0.70 and−0.60 Å for HNO_3-H_2O and $HNO_3-(H_2O)_2$, respectively.
(80) Note that the values of ρ used for the mono- and dihydrates are primarily experimental values, with only small theoretical corrections applied corresponding to the first term of eq 7. The value for the trihydrate, however, is entirely theoretical.
(81) Albinus, L.; Spieckermann, J.; Sutter, D. H. *J. Mol. Spectrosc.* **1989**, *133*, 128.
(82) Ott, M. E.; Craddock, M. B.; Leopold, K. R. *J. Mol. Spectrosc.* **2005**, *229*, 286.
(83) Adachi, A.; Kiyoyama, H.; Nakahara, M.; Masuda, Y.; Yamatera, H.; Shimizu, A.; Taniguchi, Y. *J. Chem. Phys.* **1988**, *90*, 392.
(84) Note that the 0.656 MHz value is slightly smaller than the 0.745 MHz value obtained in crystalline $NaNO_3$:Gourdji, M.; Guibe, L. C. R. *Acad. Sci. Paris* **1965**, *260*, 1131. However, the aqueous value seems more appropriate for the present comparison.
(85) Legon, A. C. *Chem. Soc. Rev.* **1993**, 153, and references therein.

JP9063033